

R. SEASHOLTZ 77-1

# HUGHES

RESEARCH LABORATORIES

RESEARCH REPORT NO. 243

**THEORY AND PERFORMANCE OF  
AUXILIARY DISCHARGE  
THERMIONIC ENERGY CONVERTERS**

R. C. KNECHTLI AND MARVIN FOX  
JUNE 1962

N66-12991

FACILITY FORM 802

(ACCESSION NUMBER)

(THRU)

39

1

(PAGES)

(CODE)

03

(NASA CR OR TMX OR AD NUMBER)

(CATEGORY)

GPO PRICE \$ \_\_\_\_\_

CFSTI PRICE(S) \$ \_\_\_\_\_

Hard copy (HC) 2.00

Microfiche (MF) .50

**LIBRARY COPY**

MAR 6 1964

LEWIS LIBRARY, NASA  
CLEVELAND, OHIO

HUGHES RESEARCH LABORATORIES  
Malibu, California

a division of hughes aircraft company

Research Report No. 243

THEORY AND PERFORMANCE OF  
AUXILIARY DISCHARGE THERMIONIC  
ENERGY CONVERTERS\*

R. C. Knechtli and Marvin Fox  
Electron Dynamics Department

June 1962

\*Supported by the National Aeronautics and Space Administration  
under Contract NAS 3-1909.

TABLE OF CONTENTS

ABSTRACT . . . . . 1

I. THEORY OF AN AUXILIARY DISCHARGE  
THERMIONIC ENERGY CONVERTER . . . . . 2

    Theoretical Assumptions . . . . . 6

    Conservation of Electrons . . . . . 6

    Conservation of Ions . . . . . 9

    Optimum Load Current Versus Auxiliary  
    Discharge Current . . . . . 12

    Maximum Load Current Versus Auxiliary  
    Discharge Current . . . . . 14

    Plasma Resistivity . . . . . 18

    Conservation of Energy and Electron  
    Temperature . . . . . 19

II. EXPERIMENTAL RESULTS . . . . . 22

    Measurements of Load Current Versus  
    Auxiliary Discharge Current . . . . . 22

    Measurements of Plasma Resistance . . . . . 29

III. CONCLUSIONS . . . . . 33

APPENDIX . . . . . 34

REFERENCES . . . . . 35

## LIST OF ILLUSTRATIONS

Fig. 1.	Schematic of the auxiliary discharge thermionic converter . . . . .	3
Fig. 2.	Potential distribution in an auxiliary discharge thermionic converter for ion sheath at collector. . . . .	4
Fig. 3.	Potential distribution in an auxiliary discharge thermionic converter for electron sheath at collector . . . . .	5
Fig. 4.	Current-voltage characteristics with auxiliary discharge current $I_a$ as a parameter . . . . .	16
Fig. 5.	Schematic of circuit for obtaining current-voltage characteristics . . . . .	23
Fig. 6.	Current-voltage characteristics of an auxiliary discharge thermionic converter . . . . .	24
Fig. 7.	Maximum load current versus auxiliary discharge current . . . . .	25
Fig. 8.	Plasma resistance versus load current . . . . .	32

Abstract

12991

A theory of auxiliary discharge thermionic energy converters is presented. Using this theory, it is possible to predict a converter's current-voltage characteristics as functions of auxiliary discharge current, auxiliary discharge voltage, and geometry. It is also possible to predict the resistive voltage drop across the plasma as a function of load current. Auxiliary discharge converter current-voltage characteristics were measured with auxiliary discharge current and voltage as parameters. These measurements are presented and compared with theoretical predictions. Quantitative agreement between theory and experiment has been obtained so far. In particular, the relatively low auxiliary discharge currents and low auxiliary discharge powers observed in the experiments appear consistent with theory.

*Author*

## I. Theory of an Auxiliary Discharge Thermionic Energy Converter

### Description of Device

The physical model of the auxiliary discharge energy converter discussed in this paper consists of an emitter of area  $A_e$  facing a collector of area  $A_c$ , the two surfaces being parallel and separated by a distance  $d$  of the order of a millimeter. In the mid-plane between these electrodes there is a thin wire configuration which serves as an auxiliary electron emitter. This system operates in an atmosphere of a noble gas at a pressure  $p$  of the order of 1 Torr. The auxiliary electron emitter is made negative by a potential  $V_a$ , with respect to the main electrodes. With  $V_a$  slightly larger than the ionization potential of the noble gas, a Langmuir mode discharge is created between the auxiliary emitter and the other electrodes. This auxiliary discharge economically provides the positive ions required for the space-charge neutralization of the load current flowing between the main electrodes. General discussion of the advantages and of the optimum operating conditions (temperature) for good efficiency of such an auxiliary discharge thermionic energy converter can be found in prior publications.<sup>1,2</sup> The purpose of this paper is to present a more detailed theoretical and experimental treatment of the gas discharge processes and plasma characteristics of this type of device. Of particular significance will be the theoretical and experimental determination of the required auxiliary discharge power, and of the plasma resistance or plasma potential drop.

A schematic of the system considered is shown in Fig. 1. The potential distributions of practical interest correspond to space-charge-limited operation of the main emitter and are shown in Figs. 2 and 3. Figures 2(a) and 3(a) depict the potential in a plane perpendicular to the main electrodes, where it is not perturbed by the auxiliary emitter. Figures 2(b) and 3(b) show the potential distribution in a similar plane passing through an auxiliary emitting wire. It will be shown that the

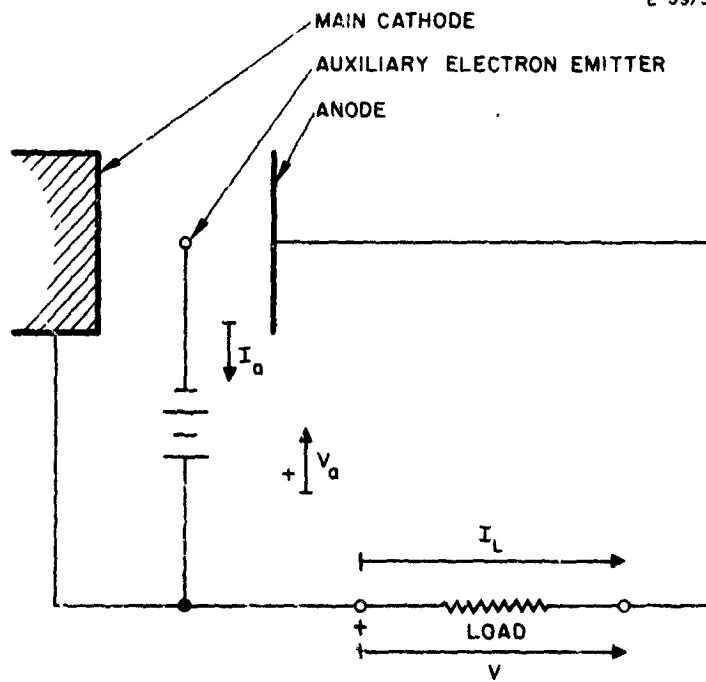


Fig. 1 Schematic of the auxiliary discharge thermionic converter.

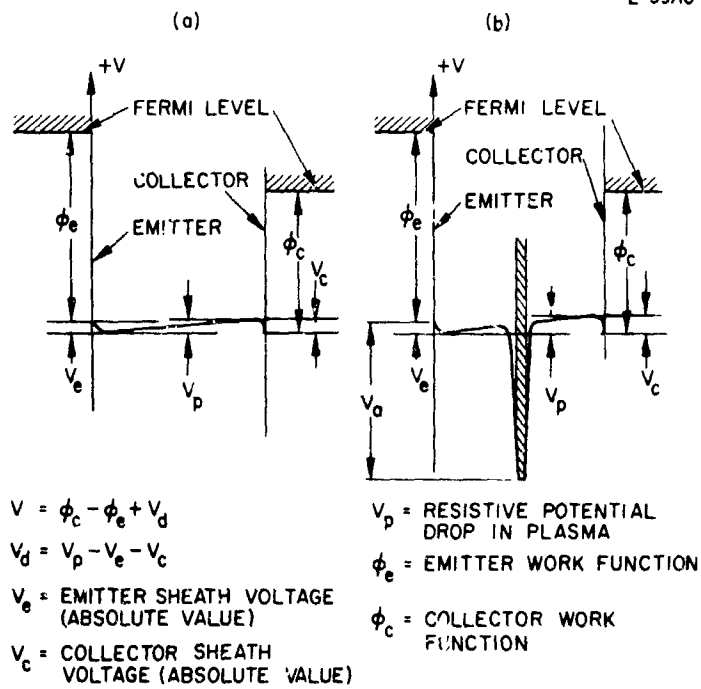


Fig. 2. Potential distribution in an auxiliary discharge thermionic converter for ion sheath at collector.

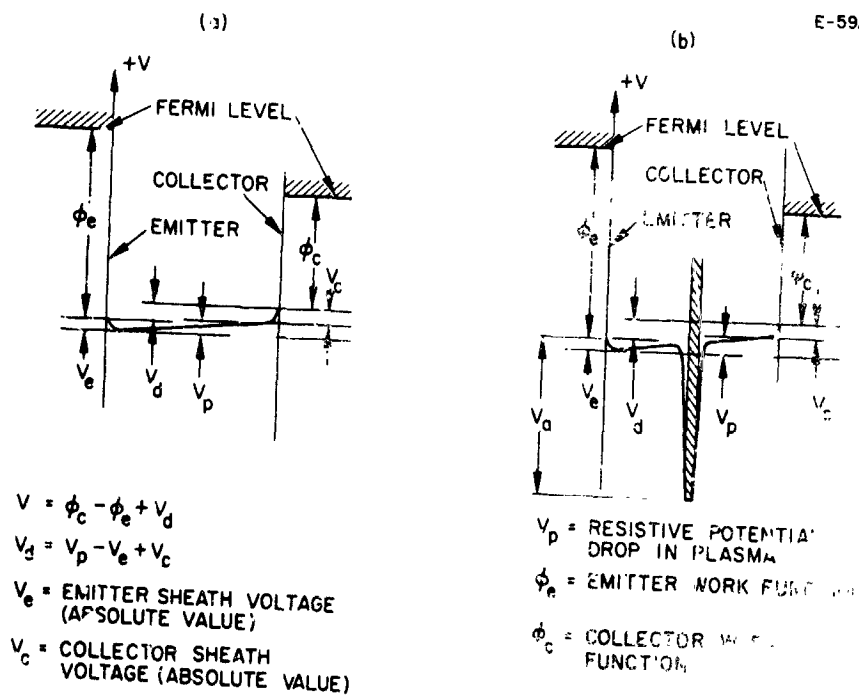


Fig. 3. Potential distribution in an auxiliary discharge thermionic converter for electron sheath at collector.

transition from the potential distribution of Fig. 2 to that of Fig. 3 occurs with increasing load current; the transition condition between Fig. 2 and Fig. 3 (zero collector sheath) will be seen to correspond approximately to the most favorable operating conditions of the converter. In order to determine the converter's I-V (current-voltage) characteristics as functions of auxiliary discharge current and of geometry, it is necessary to determine the sheath potentials as functions of these parameters. This will now be done by using the conditions of conservation of electrons and of ions.

#### Theoretical Assumptions

The following assumptions are made for the analysis given below:

1. Uniform electron and ion density outside of sheaths (i. e., density independent of position in plasma).
2. Uniform electron temperature (i. e., electron temperature independent of position).

While it will be apparent from the equation of conservation of energy that the assumption of uniform electron temperature is not rigorously correct, this assumption still remains an acceptable approximation because the actual electron temperature gradients will be seen to be relatively small. The assumption of uniform electron density also is not rigorously correct. However, because ion generation is relatively uniform throughout the plasma volume and because the ion sinks also are relatively uniformly distributed (main electrodes, auxiliary emitter, and side of gap between main electrodes), the assumption of uniform density is expected to be reasonably good.

#### Conservation of Electrons

Under the above approximations and with the potential distribution shown in Fig. 2, the condition for the conservation of electrons becomes

$$A_e J_{e0} \exp \left[ -\frac{e V_0}{k T_e} \right] = \left\{ A_e + A_c \exp \left[ -\frac{e V_c}{k T_e} \right] \right\} \left( \frac{e n_e \bar{v}_e}{4} \right), \quad (1)$$

where

- $A_e \equiv$  main emitter area
- $A_c \equiv$  main collector area
- $J_{e\epsilon} \equiv$  electron saturation current density at main emitter
- $V_e \equiv$  main emitter sheath voltage (absolute value)
- $V_c \equiv$  collector sheath voltage (absolute value)
- $e \equiv$  electronic charge
- $k \equiv$  Boltzmann constant
- $T_\epsilon \equiv$  electron temperature
- $n_\epsilon \equiv$  electron density in plasma
- $\bar{v}_\epsilon \equiv$  mean (thermal) electron velocity

The load current  $I_L$  equals the electron current reaching the collector and, for a Maxwellian electron velocity distribution, is given by

$$I_L = \left( \frac{e n_\epsilon \bar{v}_\epsilon}{4} \right) \left\{ A_c \exp \left[ - \frac{e V_c}{k T_\epsilon} \right] \right\}, \quad (2)$$

the emitter saturation current is

$$I_s = A_e J_{e\epsilon}, \quad (3)$$

and the plasma electron "random" current density is

$$J_{P\epsilon} = \frac{e n_\epsilon \bar{v}_\epsilon}{4}. \quad (4)$$

Thus eq. (1) can be rewritten in the simplified form

$$I_s \exp \left[ - \frac{e V_e}{k T_\epsilon} \right] = A_e J_{P\epsilon} + I_L. \quad (5)$$

From eqs. (1) and (2), it follows that

$$V_e = \left( \frac{k T \epsilon}{\epsilon} \right) \ln \left( \frac{I_s}{A_e J_{P\epsilon} + I_L} \right) \quad (6)$$

and

$$V_c = \left( \frac{k T \epsilon}{\epsilon} \right) \ln \left( \frac{A_c J_{P\epsilon}}{I_L} \right) . \quad (7)$$

From eqs. (3) and (4), the conditions under which the potential distribution in Fig. 2 exists are seen to be defined by

$$I_s \geq A_e J_{P\epsilon} + I_L \quad (8)$$

and

$$I_L < A_c J_{P\epsilon} . \quad (9)$$

It will be seen later that the requirements (8) and (9) should usually be satisfied for practical operating conditions. With eqs. (6) and (7), it now is possible to write the complete relation between the collector-emitter voltage  $V$  and the load current  $I_L$ . This voltage  $V$  is defined as the electrostatic potential difference between the Fermi levels of the collector and the emitter with  $V < 0$  for generator operation:

$$V = (\phi_c - \phi_e) + I_L R_P - \frac{k T \epsilon}{\epsilon} \ln \left( \frac{I_s}{I_L} \frac{A_e J_{P\epsilon}}{A_c J_{P\epsilon} + I_L} \right), \quad (10)$$

where  $R_P$  is the plasma resistance. Equation (10) will be used in the evaluation of experimental results to determine the plasma resistance  $R_P$  from the slope  $dV/dI$  and the current  $I$  of the I-V characteristic in that part of the characteristic where the potential distribution of Fig. 2 applies, i. e., where eqs. (8) and (9) are satisfied.

### Conservation of Ions

In eq. (10), which determines the I-V characteristic of an auxiliary discharge converter, the random electron plasma current density  $J_{pe}$  still is an unknown. Therefore, to completely determine the I-V characteristic, an additional relation between  $J_{pe}$  and the load current is required. This relation will be supplied as a function of auxiliary discharge parameters and geometry by the condition of conservation of ions together with the condition for plasma neutrality.

The condition for conservation of ions states that the rate of ion generation equals the rate of ion loss. The rate of ion generation is

$$\left. \frac{\partial N}{\partial t} \right|_+ = \nu (p P_i l) \frac{I_a}{\epsilon} , \quad (11)$$

where

$\nu \equiv$  ratio of cross section for ionization to total inelastic collision cross section

$p \equiv$  gas pressure, Torr

$P_i \equiv$  ionization "probability" (normalized)

$l \equiv$  effective length of electron trajectory for ionization, cm

$I_a \equiv$  auxiliary discharge current, amperes.

For the potential distribution in Fig. 2, the rate of ion loss is given by

$$\left. \frac{\partial N}{\partial t} \right|_- = n_p \left\{ \underbrace{\frac{\bar{v}_{pc}}{4} A_c}_{\text{loss on collector}} + \underbrace{\frac{\bar{v}_{pa}}{4} A_a}_{\text{loss on auxiliary emitter}} + \underbrace{\frac{\bar{v}_{pg}}{4} A_g}_{\text{loss by diffusion through side of gap between collector and main emitter}} + \underbrace{\frac{\bar{v}_{pe}}{4} A_e}_{\text{loss on main emitter}} \exp \left[ -\frac{\epsilon V_e}{kT_{pe}} \right] \right\} , \quad (12)$$

where

- $n_p$   $\equiv$  positive ion density in plasma, outside of pre-sheaths
- $\bar{v}_{pc}$   $\equiv$  ion mean thermal velocity in vicinity of collector
- $\bar{v}_{pe}$   $\equiv$  ion mean thermal velocity in vicinity of emitter
- $\bar{v}_{pg}$   $\equiv$  ion mean thermal velocity in vicinity of side of gap
- $T_{pe}$   $\equiv$  ion temperature in vicinity of main emitter
- $A_g$   $\equiv$  area of side of gap between collector and main emitter;  
for disk-shaped emitter and collector of radius R and  
separation d,  $A_g = 2\pi Rd$ .

Because of the planar geometry of main emitter and collector, the ion drift toward these electrodes is essentially one dimensional; the pre-sheath area, the sheath area, and the electrode area are approximately equal. Hence, with  $n_p$  being the ion density in the plasma outside of the pre-sheath, it is appropriate to use the true mean thermal ion velocities in the plasma, as defined above, to express the rates of ion loss at the collector and at the main emitter in eq. (12).

At the auxiliary emitter, however, a cylindrical geometry and converging ion drift motion exist. Therefore, if  $A_a$  is the "effective" auxiliary emitter area, defined as the area of the sheath around the auxiliary emitter, the effect of the electric fields of the pre-sheath on the ion drift toward the auxiliary emitter has to be taken into account. This can be done by defining  $\bar{v}_{pa}$  as an "effective" ion mean thermal velocity corresponding to the electron temperature rather than to the ion temperature.<sup>3</sup> For this reason,  $\bar{v}_{pa}$  and  $A_a$  are defined as follows, for eq. (12) and ff.:

- $\bar{v}_{pa}$  = "effective" ion mean thermal velocity at auxiliary emitter sheath edge, equal to the ion mean thermal velocity corresponding to the electron temperature
- $A_a$  = "effective" auxiliary emitter area, equal to the sheath area.

Expressing the condition of conservation of ions by equating the right members of eq. (11) and (12), taking  $\bar{v}_{pg} \cong \bar{v}_{pc}$ , substituting  $\bar{v}_{pe}/\bar{v}_{pc} = T_{pe}/T_{pc}$  and  $\bar{v}_{pa}/\bar{v}_{pc} \cong T_e/T_{pc}$ , and solving for  $n_p$  leads to

$$n_p \approx \frac{\nu_p P_i l I_a}{\epsilon \left(\frac{\bar{v}_{pc}}{4}\right) \left\{ A_c + A_g + A_a \sqrt{\frac{T_\epsilon}{T_{pc}}} + A_e^- \sqrt{\frac{T_{pe}}{T_{pc}}} \exp \left[ -\frac{\epsilon V_e}{k T_{pe}} \right] \right\}}, \quad (13)$$

where  $T_{pc}$  is the ion temperature in vicinity of collector.

Equation (13) may be re-written in terms of the random plasma electron current  $I_{Pc} = A_c J_{Pe} = A_c (\epsilon n_e \bar{v}_e / 4)$  available at the collector sheath by using the condition for plasma neutrality  $n_p = n_e$ . Substituting also  $\bar{v}_{pc} / \bar{v}_e = \sqrt{T_{pc} M_e / T_e M_p}$  leads from eq. (13) to

$$\frac{I_{Pc}}{I_a} = \frac{\nu_p P_i l \sqrt{\frac{T_\epsilon}{T_{pc}} \frac{M_p}{M_e}}}{1 + \frac{A_g}{A_c} + \sqrt{\frac{T_\epsilon}{T_{pc}}} \frac{A_a}{A_c} + \sqrt{\frac{T_{pe}}{T_{pc}}} \frac{A_e}{A_c} \exp \left[ -\frac{\epsilon V_c}{k T_{pe}} \right]}. \quad (14)$$

$V_e$  can be eliminated from eq. (14) by means of eq. (6). This yields with

$$A_e J_{Pe} = \frac{A_e}{A_c} I_{Pc},$$

$$\frac{I_{Pc}}{I_a} = \frac{\nu_p P_i l \sqrt{\frac{T_\epsilon}{T_{pc}} \frac{M_p}{M_e}}}{1 + \frac{A_g}{A_c} + \sqrt{\frac{T_\epsilon}{T_{pc}}} \frac{A_a}{A_c} + \sqrt{\frac{T_{pe}}{T_{pc}}} \frac{A_e}{A_c} \left[ \frac{I_L}{I_s} \left( 1 + \frac{I_{Pc}}{I_L} \frac{A_e}{A_c} \right) \right]^{T_\epsilon / T_{pe}}}. \quad (15)$$

Equations (10) and (15) constitute a set of two parametric equations with  $J_{Pe}$  and  $I_{Pc} = A_c J_{Pe}$ , respectively, as parameters; these equations uniquely determine the relation between the converter voltage  $V$

and the load current  $I_L$  (I-V characteristic) when the conditions of eqs. (8) and (9) are satisfied (potential distribution of Fig. 2). This system of two equations could be solved numerically by computer to yield families of complete I-V characteristics. Rather than doing this, however, it is more useful to relate analytically the load current  $I_L$  to the auxiliary discharge current  $I_a$  for specific and characteristic operating points on the I-V characteristic, choosing these points to be of practical significance. This will be done in the next section.

#### Optimum Load Current Versus Auxiliary Discharge Current

The optimum load current at which it is desirable to operate the type of converter discussed in this paper is approximately that corresponding to zero collector sheath voltage.\* It is therefore of interest to evaluate the load current  $I_{Lo}$  corresponding to zero collector sheath voltage as a function of auxiliary discharge current. The load current  $I_{Lo}$  for zero collector sheath voltage is given by

$$I_{Lo} = A_c J_{Pe0} = I_{Po} , \quad (16)$$

where

$$J_{Pe0} \equiv \text{value of } J_{Pe} \text{ for } V_c = 0$$

$$I_{Po} \equiv \text{value of } I_{Pc} \text{ for } V_c = 0.$$

By introducing eq. (16) into eq. (15), the following expression is found for  $I_{Lo}$ :

---

\* It will be shown farther on that making the collector positive with respect to the plasma (potential distribution of Fig. 3) reduces the rate of ion loss because of ion reflection at the collector sheath. The penalty paid for this advantage is however a loss of generator voltage which tends to off-set the improvement of auxiliary discharge efficiency gained by operating with such a potential distribution.

$$\frac{I_{Lo}}{I_a} = \frac{\nu p P_i l \sqrt{\frac{M_p}{M_e} \frac{T_\epsilon}{T_{pc}}}}{1 + \frac{A_g}{A_c} + \sqrt{\frac{T_\epsilon}{T_{pc}} \frac{A_a}{A_c}} + \sqrt{\frac{T_{pe}}{T_{pc}} \frac{A_e}{A_c}} \left[ \frac{I_{Lo}}{I_s} \left( 1 + \frac{A_e}{A_c} \right) \right]^{T_\epsilon/T_{pe}}}. \quad (17)$$

Because the point where  $V_c = 0$  is not readily identified on an experimental I-V characteristic, eq. (17) is not particularly useful for experimental verification of the present theory. Another equation relating the load current to the auxiliary discharge current at an experimentally identifiable point will therefore be derived later. However, because  $I_{Lo}$  is in the vicinity of the optimum load current for maximum efficiency, it is of interest to use eq. (17) for a theoretical prediction of the corresponding power consumption of the auxiliary discharge.

As a numerical example for eq. (17), we specify the following typical numerical values corresponding to operations with argon gas at optimum pressure (about 2 Torr for a 1-mm spacing between main emitter and collector):

$$\left. \begin{array}{l} \nu = 0.4 \\ p P_i l = 1 \end{array} \right\} \begin{array}{l} \text{which means that the gas pressure is high enough} \\ \text{for practically all auxiliary discharge electrons to} \\ \text{to experience one inelastic collision before being} \\ \text{collected} \end{array}$$

$$A_g/A_c = 0.05 \quad \text{for } A_c = 20 \text{ cm}^2 \text{ and } A_g = 1 \text{ cm}^2$$

$$A_e/A_c = 0.5 \quad \text{for } A_e = 10 \text{ cm}^2$$

$$A_a/A_c = 0.1$$

$$T_\epsilon = 2000^\circ\text{K}$$

$$T_{pc} = 750^\circ\text{K}$$

$$T_{pe} = 1500^\circ\text{K}$$

$$\frac{I_s}{I_{Lo}} = 1 + \frac{A_e}{A_c} = 1.5; \quad I_{Lo} = \frac{2}{3} I_s; \quad \sqrt{\frac{M_p}{M_e}} = 270 \text{ for argon.}$$

Under these conditions, which prevail at an auxiliary discharge voltage of about 20 V in argon, eq. (15) yields

$$\frac{I_{Lo}}{I_a} \approx \frac{(0.4)(270)(1.6)}{1 + 0.05 + 0.16 + \frac{\sqrt{2}}{2}} = 90 .$$

The corresponding auxiliary discharge power expenditure is

$$P_a = I_a V_a = V_a I_{Lo} \left( \frac{I_a}{I_{Lo}} \right).$$

Normalized in terms of watts per ampere of load current,

$$\frac{P_a}{I_{Lo}} = \frac{V_a}{\frac{I_{Lo}}{I_a}} = \frac{20}{90} \approx 0.2 \text{ W/A} .$$

This figure, obtained for argon with realistic design parameters, is acceptably low. It can be reduced further by a factor of about 2 by substituting xenon for argon, because of the higher mass and lower ionization potential of xenon.

#### Maximum Load Current Versus Auxiliary Discharge Current

A quantity readily identified on an experimental I-V characteristic is the maximum load current  $I_L^{\max}$  which can flow for a given auxiliary discharge current  $I_a$ . In order to verify experimentally the present theory, it is necessary to predict the theoretical value of  $I_L^{\max}/I_a$  as a function of the saturation current  $I_s$  available at the emitter and to compare this theoretical prediction with measurements.

As the converter voltage  $V$  is increased,\* starting from open circuit with the potential distribution of Fig. 2, the collector sheath

\*According to our sign conventions, increasing  $V$  may mean decreasing absolute value of load voltage, because  $V < 0$  for generator operation (see Figs. 2 and 3).

voltage decreases in absolute value, becomes zero, and changes sign to result in a potential distribution of the type shown in Fig. 3. As the collector becomes positive with respect to the plasma, ions from the plasma are reflected by the collector sheath. This tends to reduce the rate of ion loss and, for constant auxiliary discharge current, thus increases the plasma density. As the collector voltage is increased further, the ion loss on the collector becomes negligible and the plasma density becomes maximum and independent of further voltage increases. This results in a family of I-V characteristics of the type shown in Fig. 4. The maximum load current for a given auxiliary discharge current corresponds to the maximum attainable plasma density because the load current equals the total random plasma current available at the collector as soon as the collector potential exceeds the plasma potential. Thus  $I_L^{\max}$  corresponds to negligible ion loss on the collector. The rate of ion loss then is found by suppressing the first term in the right member of eq. (12). The corresponding plasma density is found by suppressing the term  $A_c$  in the denominator of the right member of eq. (13). Since the maximum load current is equal under these conditions to the random plasma current  $I_{Pc}$ ,  $I_L^{\max}$  is found by substituting  $I_L^{\max} = I_{Pc}$  in eq. (15) and suppressing the first term of the denominator of the right member of this same equation. This yields

$$\frac{I_L^{\max}}{I_a} = \frac{\nu_p P_i \sqrt{\frac{M_p T_e}{M_e T_{pc}}}}{\frac{A_g}{A_c} + \sqrt{\frac{T_e}{T_{pc}}} \frac{A_a}{A_c} + \sqrt{\frac{T_{pe}}{T_{pc}}} \frac{A_e}{A_c} \left[ \frac{I_L^{\max}}{I_s} \left( 1 + \frac{A_e}{A_c} \right) \right]^{T_e/T_{pe}}}. \quad (18)$$

This equation will be used in Section II for comparison with experimental results. It is of further interest to compare eqs. (17) and (18) to determine in which part of an I-V characteristic the potential distribution corresponds to Fig. 2 and in which part it corresponds to Fig. 3. By definition of  $I_{Lo}$  (load current for zero collector sheath

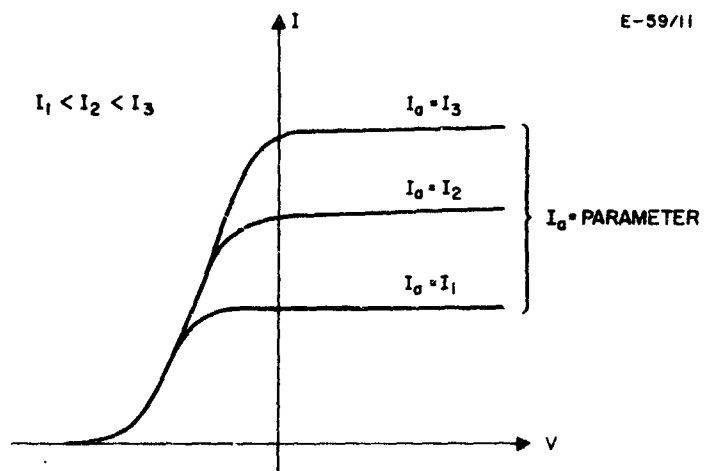


Fig. 4. Current-voltage characteristics with auxiliary discharge current  $I_a$  as a parameter.

voltage), the potential distribution corresponds to Fig. 2 for  $I_L < I_{Lo}$  and to Fig. 3 for  $I_L > I_{Lo}$ . Because  $I_L^{\max}$  is directly measurable, it is of interest to express  $I_{Lo}$  as a function of  $I_L^{\max}$ . From eqs. (17) and (18),

$$\frac{I_{Lo}}{I_L^{\max}} = \frac{\frac{A_g}{A_c} + \sqrt{\frac{T_\epsilon}{T_{pc}}} \frac{A_a}{A_c} + \sqrt{\frac{T_{pe}}{T_{pc}}} \frac{A_e}{A_c} \left[ \frac{I_L^{\max}}{I_s} \left( 1 + \frac{A_e}{A_c} \right) \right]^{T_\epsilon/T_{pe}}}{1 + \frac{A_g}{A_c} + \sqrt{\frac{T_\epsilon}{T_{pc}}} \frac{A_a}{A_c} + \sqrt{\frac{T_{pe}}{T_{pc}}} \frac{A_e}{A_c} \left[ \frac{I_{Lo}}{I_s} \left( 1 + \frac{A_e}{A_c} \right) \right]^{T_\epsilon/T_{pe}}} \quad (19)$$

This equation can be solved by numerical or graphical methods. In the case where

$$I_L^{\max} < \frac{I_s}{1 + \frac{A_e}{A_c}}$$

and

$$\frac{A_e}{A_c} \leq 1,$$

an approximate analytical solution is obtained by observing that  $I_{Lo} < I_L^{\max}$  and  $T_\epsilon > T_{pe}$ , which makes

$$\frac{A_e}{A_c} \left[ \frac{I_{Lo}}{I_s} \left( 1 + \frac{A_e}{A_c} \right) \right]^{T_\epsilon/T_{pe}} \ll 1.$$

Because  $\sqrt{T_{pe}/T_{pc}} \leq 2$  in practical cases, eq. (19) then can be simplified as follows:

$$\frac{I_{L0}}{I_L^{\max}} \approx \frac{\frac{A_g}{A_c} + \sqrt{\frac{T_e}{T_{pc}}} \frac{A_a}{A_c} + \sqrt{\frac{T_{ps}}{T_{pc}}} \frac{A_e}{A_c} \left[ \frac{I_L^{\max}}{I_s} \left( 1 + \frac{A_e}{A_c} \right) \right]^{T_e/T_{pe}}}{1 + \frac{A_g}{A_c} + \sqrt{\frac{T_e}{T_{pc}}} \frac{A_a}{A_c}} \quad (19a)$$

Equation (19) and/or (19a) will be useful in determining the region in experimental I-V characteristics (i. e.,  $I_L \leq I_{L0}$ ) to which eqs. (10) and (15) apply. This will be of particular interest in Section II for the evaluation of the plasma resistance  $R_p$  from experimental I-V characteristics.

#### Plasma Resistivity

There are two contributions to the plasma resistivity  $\rho$ : that arising from the electron-neutral collisions  $\rho_{e0}$ , and that resulting from the electron-ion collisions  $\rho_{ep}$ . Thus

$$\rho = \rho_{e0} + \rho_{ep} \quad (20)$$

In applications of practical interest and in the experiments reported below, noble gases exhibiting the Ramsauer effect are used. The electron-neutral mean free path then is relatively long and is equal to or larger than the emitter-collector spacing. For this reason, the contribution of  $\rho_{e0}$  is relatively unimportant and will be neglected henceforth.

The electron-ion mean free path however may be shorter than the distance between emitter and collector. The quantity  $\rho_{ep}$  then can be evaluated from Spitzer's equation<sup>5</sup>

$$\rho_{ep} = \frac{6.53 \times 10^3 \ln \Lambda}{T_e^{3/2}} \Omega\text{-cm} ,$$

where  $\ln \Lambda \approx 6$  (slowly varying function of  $n_e$  and  $T_e$ ). Hence

$$\rho \approx \rho_{ep} = \frac{39 \times 10^3}{T_e^{3/2}} \Omega\text{-cm} . \quad (21)$$

Values derived from eq. (21) will be compared with experimental results for the plasma resistivity.

### Conservation of Energy and Electron Temperature

It is seen in eq. (21) that the electron temperature is of predominant importance in determining the plasma resistivity; it is also of importance in determining sheath potentials and I-V characteristics (see eq. (10)). The electron temperature will therefore be evaluated. To this end, the equation of conservation of energy is written for the electrons in the plasma between emitter and collector sheaths. This equation states that the electron energy flow into the plasma equals the electron energy flow out of the plasma. The assumptions made in this derivation are as follows:

1. Negligible energy transfer from electrons to ions or neutrals.
2. Near Maxwellian electron velocity distribution, characterized by a temperature  $T_e(x)$ , which is a function of distance  $x$  from the emitter sheath.
3. Negligible energy transfer between fast electrons of the auxiliary discharge and slow electrons from the main emitter.

Under these conditions, the power flow into the plasma between  $x = 0$  and  $x = x$  is, for the potential distribution in Fig. 2,

$$P_{in} = I_{in} \left( \frac{2k T_e}{e} \right) + I_L V(x) ; \quad (22)$$

where

$I_{in} \equiv$  the electron current injected into the plasma through the emitter sheath

$T_e \equiv$  the electron temperature at the emitter sheath and is equal to the emitter temperature

$V(x) \equiv$  the difference in plasma potential between the edge of the emitter sheath (plane  $x = 0$ ) and the plane  $x = x$  at which the electron temperature  $T_e(x)$  is evaluated;  $V(x)$  is the potential difference needed to maintain the flow of the load current  $I_L$  through the plasma resistance existing between the planes 0 and  $x$ .

The power flow out of the plasma is

$$P_{out} = I_{Pe} \left( \frac{2k T_e}{e} \right) + I_L \left( \frac{2k T_e(x)}{e} \right) ,$$

where  $I_{Pe}$  is the random plasma electron current returning from the plasma to the emitter through the emitter sheath.

The equation of conservation of electrons states that

$$I_{in} \cong I_{Pe} + I_L .$$

Equating these power flows,  $P_{in}$  and  $P_{out}$ , and eliminating  $I_{in}$  by means of this last equation leads to

$$\frac{k T_e(x)}{e} = \frac{k T_e}{e} + \frac{V(x)}{2} . \quad (23)$$

In particular, the electron temperature  $T_{\epsilon C}$  at the collector is\*

$$\frac{k T_{\epsilon C}}{\epsilon} = \frac{k T_e}{\epsilon} + \frac{V_P}{2} . \quad (24)$$

Because the temperature difference  $\Delta T = T_{\epsilon C} - T_e$  will be seen to be smaller in general than  $T_e$ , it is legitimate to use for the present considerations an average electron temperature  $T_\epsilon$  defined by

$$T_\epsilon = \frac{1}{2} (T_e + T_{\epsilon C}) .$$

According to this definition and to the above equations

$$T_\epsilon = T_e + \left(\frac{\epsilon}{k}\right) \frac{V_P}{4} . \quad (25)$$

This value of  $T_\epsilon$  given by eq. (25) can be introduced into eq. (21) to obtain a first order approximation for the plasma resistance between emitter and collector. It also can be introduced into eq. (10) for a first order evaluation of I-V characteristics and into eqs. (17) and (18) for an evaluation of the relation between load current and auxiliary discharge current.

---

\*A more rigorous derivation would be obtained by defining  $T_\epsilon$  as the temperature of electrons drifting with an average velocity  $u$ , the velocity distribution being Maxwellian in the frame of reference moving at this velocity  $u$ . Defining  $u_0$  and  $u_x$  as the values of  $u$  at the planes 0 and  $x$ , respectively, we would then obtain instead of eq. (23)

$$\frac{k T_\epsilon(x)}{\epsilon} = \frac{k T_e}{\epsilon} + \frac{2}{3} V(x) - \frac{M_\epsilon}{3e} \left( u_x^2 - u_0^2 \right) . \quad (23a)$$

The difference between eq. (23) and (23a) results from the difference in the definition of  $T_\epsilon$  for the derivation of these two equations. For the derivation of eq. (23),  $T_\epsilon$  is an equivalent temperature representing the total kinetic energy contained in both the random and the drift motion of the electrons. This definition, although somewhat artificial, is more suitable to the present approximate theory than the more rigorous definition leading to eq. (23a).

## II. Experimental Results

### Measurements of Load Current Versus Auxiliary Discharge Current

The measurements reported here were performed with auxiliary discharge converter experimental tubes having Philips "B" dispenser emitters with an area of  $1.3 \text{ cm}^2$  and molybdenum collectors of the same area. The spacings between the main electrodes were set at 2 or 2.5 mm for each of the several tubes investigated. The auxiliary electron emitter was a 0.005-inch tungsten wire, with an area of approximately  $0.12 \text{ cm}^2$ , shaped somewhat like a sine wave; it was located in the central plane between the electrodes. The tube atmosphere was argon (ionization potential 15.7 V) at a pressure of 0.8 Torr. The auxiliary discharge voltage  $V_a$  was kept fixed at 20 V.

The data were taken from families of I - V characteristics, recorded on film, obtained with the circuit shown schematically in Fig. 5. All three electrodes could be heated with 60-cycle ac or half-wave 60-cycle ac. The sweep voltage in the load circuit also could be either full-wave or half-wave 60-cycle ac of controllable voltage. When the sweep voltage was half-wave, it was  $180^\circ$  out of phase with the half-wave voltages on the electrode heaters.

The Philips cathodes were operated at around  $1200^\circ\text{C}$ , and load currents higher than 30 A were sometimes recorded. The collector temperatures were held such as to keep back-emission negligible. A typical family of I - V characteristics is shown in Fig. 6 for a tube with 2.5-mm spacing. From these curves the maximum load current  $I_L^{\text{max}}$  corresponding to each auxiliary discharge current  $I_a$  is plotted as a function of the auxiliary discharge current in the lower curve in Fig. 7. The upper curve in Fig. 7 is for a similar set of data on a tube with a 2-mm interelectrode spacing and a larger emitter saturation current.

To compare these experimental data with theory, the theoretical values of  $I_L^{\text{max}}/I_a$  predicted for the experimental conditions are obtained by means of eq. (18), which yields, for  $A_e = A_c$

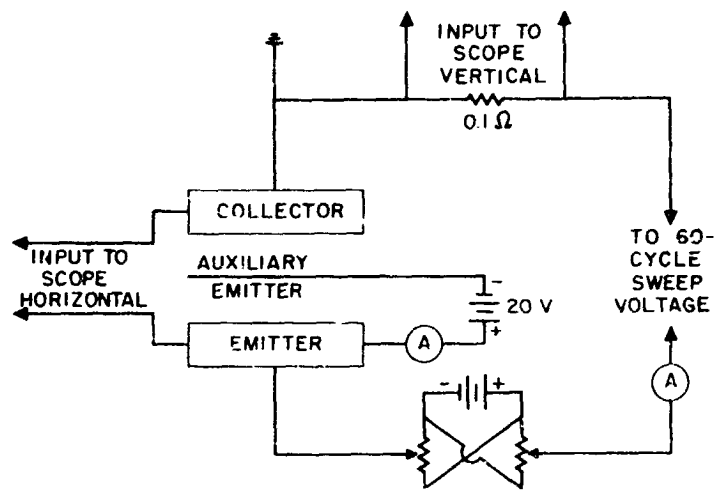


Fig. 5. Schematic of circuit for obtaining current-voltage characteristics.

E-59/R

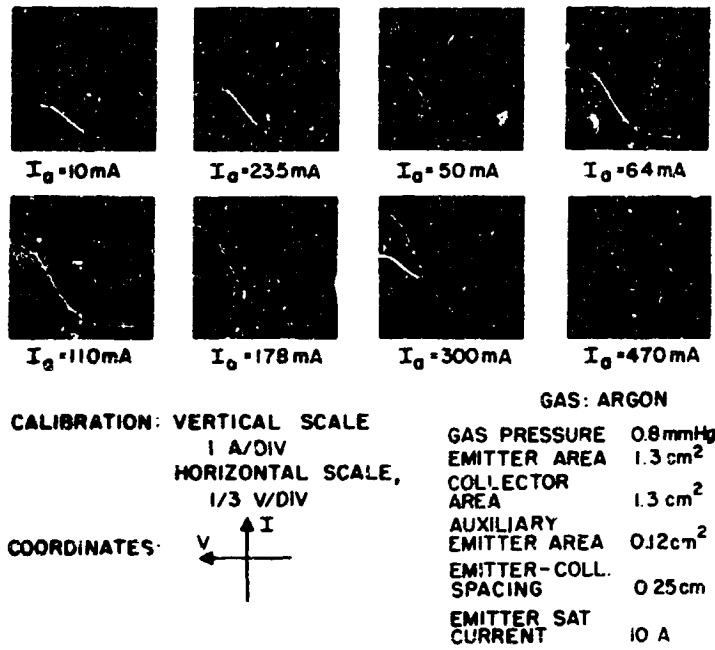


Fig. 6. Current-voltage characteristics of an auxiliary discharge thermionic converter.

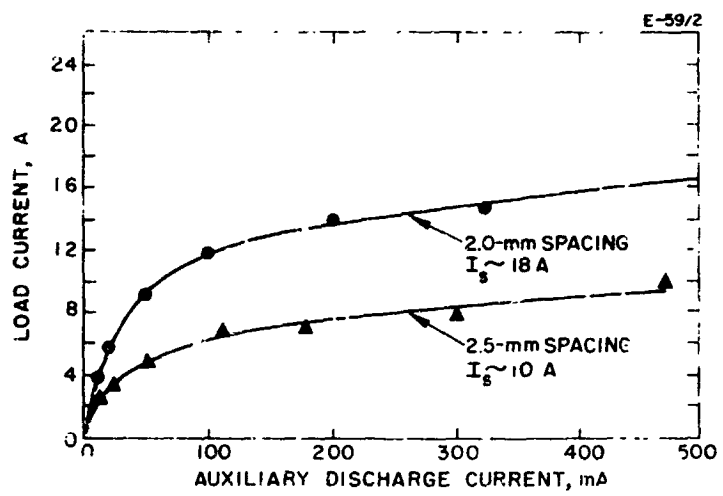


Fig. 7. Maximum load current versus auxiliary discharge current.

$$\lim \left( \frac{I_L^{\max}}{I_a} \right)_{I_a \rightarrow 0} = \frac{\nu p P_i l \sqrt{\frac{M_p}{M_\epsilon} \frac{T_\epsilon}{T_{pc}}}}{\frac{A_g}{A_c} + \sqrt{\frac{T_\epsilon}{T_{pc}} \frac{A_a}{A_c}}}$$

and

$$\left( \frac{I_L^{\max}}{I_a} \right)_{I_L^{\max} = 1/2 I_s} = \frac{\nu p P_i l \sqrt{\frac{M_p}{M_\epsilon} \frac{T_\epsilon}{T_{pc}}}}{\frac{A_g}{A_c} + \sqrt{\frac{T_\epsilon}{T_{pc}} \frac{A_a}{A_c}} + \sqrt{\frac{T_{pe}}{T_{pc}}}}$$

The following numerical values are introduced into these equations in accordance with the conditions of our experiments:

$$\left. \begin{aligned} \nu &= 0.4 \\ (p P_i l) &= 1 \quad (p = 0.8 \text{ Torr}; P_i = 3, \\ \sqrt{\frac{M_p}{M_\epsilon}} &= 270 \end{aligned} \right\} \text{for argon at a discharge voltage of 20 V}$$

$$\begin{aligned} T_{pc} &\approx 500^\circ\text{K} \\ T_\epsilon &\approx 2000^\circ\text{K} \\ T_{pe} &\approx 1000^\circ\text{K} \\ A_g &= 0.8 \text{ cm}^2 \text{ for } d = 2 \text{ mm}; \quad 1 \text{ cm}^2 \text{ for } d = 2.5 \text{ mm} \\ A_c &= A_e = 1.3 \text{ cm}^2 \\ A_a &\approx 0.16 \text{ cm}^2. \end{aligned}$$

The value of  $l$  implicitly taken above is substantially larger than the distance between the auxiliary emitter and the other electrodes because of random walk caused by elastic scattering of the auxiliary discharge

electrons by the neutral gas. The mean free path for elastic collisions of electrons at 20 eV with argon atoms at 0.8 Torr is indeed only about 0.2 mm. The probability for an auxiliary discharge electron to make an inelastic collision thus is about unity, which is expressed by taking  $pP_i l = 1$  with  $\nu = 0.4$ .

The value of  $T_e \sim 2000^\circ\text{K}$  is higher than the emitter temperature  $T_e \sim 1500^\circ\text{K}$  because of Joule heating of the electrons in the plasma, which is consistent with eq. (25).

The values of  $P_i = 3$  and  $\nu = 0.4$  were obtained from the data of W. Bleakney<sup>6,7</sup> and by the extrapolation of the data of M. J. Druyvesteyn and F. M. Penning.<sup>8,7</sup>

The value  $A_a \simeq 0.16 \text{ cm}^2$  for the effective auxiliary emitter area includes the sheath thickness and is an average value applying for a sheath voltage of 20 V and a density between  $10^{12}$  and  $10^{13}$  ions/cm<sup>3</sup>, which is the range of plasma densities corresponding to the experimental conditions. (The area of the wire itself of the auxiliary emitter is about  $0.12 \text{ cm}^2$ .)

The values used for the ion temperature  $T_{pc}$  and  $T_{pe}$  at the collector and at the emitter, respectively, are somewhat more uncertain and are educated guesses. They are taken to be about equal to the gas temperature, which is assumed to be somewhat below the temperature of the closest electrode because the bulk of the gas is at room temperature. Thus, with an emitter temperature of  $1500^\circ\text{K}$ , the ion temperature close to the emitter is taken to be about  $1000^\circ\text{K}$ . The collector temperature being of the order of  $750^\circ\text{K}$  in these experiments, the ion temperature  $T_{pc}$  close to the collector is taken to be about  $500^\circ\text{K}$ . It is plausible that gas temperature gradients do exist within the experimental device because the neutral mean free path is much smaller than the distance between electrodes. It also is plausible that the ion and neutral gas temperatures are about equal because the ion-neutral collision mean free path is much smaller than the electrode spacing and because energy transfer in an ion-neutral collision is quite effective due to the near equal mass of the colliding particles.

The theoretical values of  $I_L^{\max}/I_a$  corresponding to  $I_a \rightarrow 0$  and to  $I_L^{\max} = 1/2 I_s$  are obtained using the above numerical values in the preceding two equations. These theoretical values are shown in Table I, where they are also compared with the experimental values obtained from the curves in Fig. 7.

TABLE I  
Comparison of Theoretical and Measured Values of  $I_L^{\max}/I_a$

Saturation Current	$I_s = 10 \text{ A}$		$I_s = 18 \text{ A}$	
Electrode Spacing	$d = 2.5 \text{ mm}$		$d = 2 \text{ mm}$	
Load Current	$I_L \text{ and } I_a \rightarrow 0$	$I_L^{\max} = 1/2 I_s$	$I_L \text{ and } I_a \rightarrow 0$	$I_L^{\max} = 1/2 I_s$
$I_L^{\max}/I_a$ (theory)	212	89	250	95
$I_L^{\max}/I_a$ (measured)	240	90	400	180

Considering the uncertainty as to the exact values of  $\nu$ ,  $T_\epsilon$ ,  $T_{pc}$  and  $T_{pe}$ , the agreement between theory and experiment for these important ratios is seen to be satisfactory, thus supporting the theory developed above and providing an adequate verification of eqs. (17) and (18).

It is seen from these results that high ratios of  $I_L^{\max}/I_a$  and of  $I_{Lo}/I_a$  are to be expected in the operation of the auxiliary discharge converter\* and are confirmed by experiments. It is seen, in particular, that it is possible to obtain under practical conditions, with argon, useful load

\*This same result applies to Gabor's auxiliary discharge converter, with minor modifications. It should account for the high values of  $I_L^{\max}/I_a$  observed by Gabor in his device, without his speculation on hypothetical reflections of slow ions from conducting walls.<sup>9</sup>

currents about 100 times larger than the auxiliary discharge current. With the auxiliary discharge voltage of 20 V used for argon, this amounts to an auxiliary discharge power expenditure of the order of 0.2 W/A of useful load current. With gases of higher atomic weight and lower ionization potential, this auxiliary discharge power can be reduced further. Earlier experiments<sup>10</sup> performed with xenon show a reduction of 50% of the auxiliary discharge power, in comparison with that needed with argon. This indicates that an auxiliary discharge power as low as 0.1 W/A of load current is feasible.

#### Measurements of Plasma Resistance

These measurements have been performed with tubes identical to those described above, except that the emitter-collector spacing was reduced to  $d = 1$  mm for some of the resistance measurements. For the tubes with  $d = 1$  mm, the auxiliary emitter consisted of a number of 0.005-in. parallel tungsten wires, spaced 1/16 in. from one another, located in the central plane between main emitter and collector, with an effective emitting area of about  $0.3 \text{ cm}^2$ ; the gas atmosphere was argon at a pressure of 2 Torr.

To obtain the plasma resistance  $R_P$  from the I-V characteristics, use was made of eq. (10). This equation provides the relation between the current  $I_L$ , the voltage  $V$ , and the plasma resistance  $R_P$ , but it has the undesirable feature of including the difference  $(\phi_c - \phi_e)$  between the collector and the emitter work functions. In order to eliminate this quantity (not directly measured in our experiments), it is possible to consider  $dV/dI$  instead of  $V$ . Defining

$$V_\epsilon \equiv \left( \frac{kT_\epsilon}{\epsilon} \right)$$

and differentiating eq. (10), with  $A_e = A_c$ , leads to\*

$$R_P = \frac{dV}{dI_L} - V_e \left( \frac{1}{I_L} + \frac{1}{I_L + I_P} \right) \cdot \left[ I_L \frac{dR_P}{dI_L} + \frac{dV_e}{dI_L} \ln \frac{I_s I_P}{I_L (I_L + I_P)} \right], \quad (26)$$

where  $I_{Pc} = I_{Pe} \equiv I_P$  for  $A_e = A_c$ . All the quantities in eq. (26) are directly obtainable from our experiments, except the normalized electron temperature  $V_e$  and the rate  $dR_P/dI_L$ . The normalized electron temperature  $V_e$  could be measured by appropriate probes in the tubes, but this has not been done yet. However,  $V_e$  can be obtained in first approximation by means of eq. (25):

$$V_e \equiv \frac{kT_e}{e} \cong E_e + \frac{1}{4} I_L R_P,$$

where

$$E_e = \frac{kT_e}{e} \equiv \text{constant} \cong 0.13 \text{ V for } T_e = 1500^\circ\text{K}.$$

$$I_L R_P = V_P.$$

The quantity  $dR_P/dI$  in eq. (26) will be obtained from the theoretical curves predicted by eq. (21). Then, from eqs. (25) and (26),

\*This differentiation is performed in assuming that  $I_P$  is independent of  $I_L$ . While this is not rigorously correct, this is an acceptable simplification for the conditions to which this theory applies and for the experimental conditions to be considered, i.e., when  $I_L \leq I_{L0}$  and  $I_{L0} < I_s (1 + A_e/A_c)$ . Inspection of eq. (15) indicates that under these conditions  $I_P$  is only a slowly varying function of  $I_L$  and that the above simplification appears admissible.

$$R_P = \frac{\frac{dV}{dI_L} - E_e \left[ \frac{2I_L + I_P}{I_L(I_L + I_P)} \right] - I_L \frac{dR_P}{dI_L} \left[ 1 + \frac{1}{4} \ln \frac{I_s I_P}{I_L(I_L + I_P)} \right]}{\frac{5}{4} + \frac{1}{4} \left[ \frac{I_L}{I_L + I_P} + \ln \frac{I_s I_P}{I_L(I_L + I_P)} \right]} \quad (27)$$

This equation will be used to obtain the plasma resistance  $R_P$  from the experimental I - V curves like those shown in Fig. 6. These experimental values of  $R_P$  are then compared with the values predicted theoretically by eq. (21). To use this latter equation, it is necessary to make the substitution

$$R_P = \frac{d}{A_c} \rho \quad ,$$

where

$d \equiv$  interelectrode spacing (2.5 mm or 1 mm)

$A_c \equiv 1.3 \text{ cm}^2$

and  $T_e$  is used as given by eq. (25). Then, from eqs. (21) and (25),

$$R_P = \frac{d}{A} \frac{0.67}{1 + 1.93 I_L R_P} \Omega \quad . \quad (28)$$

A comparison of the theoretical values of  $R_P$  derived from eq. (28) and the corresponding experimental values of  $R_P$  given by the I - V characteristics and by eq. (27) is displayed in Fig. 8 for (Curve A) an emitter-collector spacing of  $d = 2.5$  mm, an auxiliary discharge current  $I_a = 50$  mA, and a saturation emitter current  $I_s = 10$  A; (Curve B) an emitter-collector spacing  $d = 1$  mm,  $I_a = 120$  mA, and  $I_s = 35$  A.

In view of the rather crude assumptions upon which the theory is based, agreement between theory and experiment is seen to be adequate.

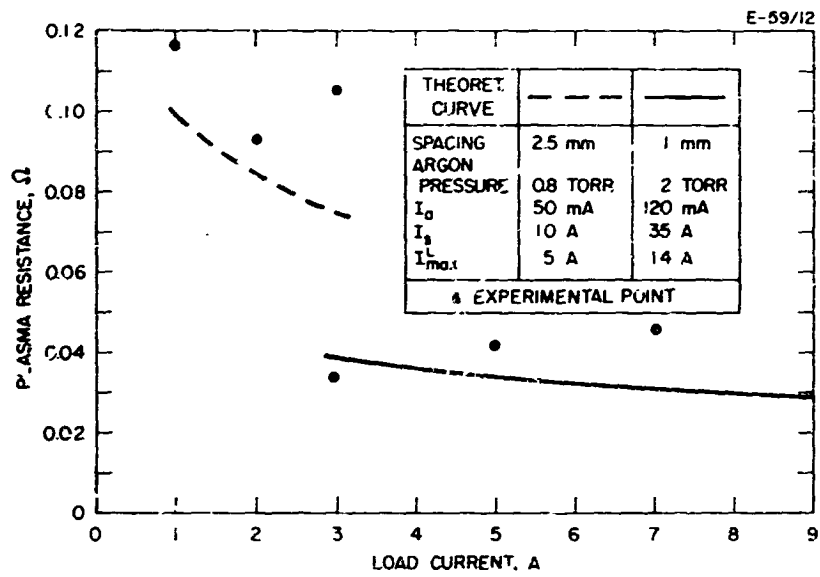


Fig. 8. Plasma resistance versus load current.

### III. Conclusions

The above theoretical as well as experimental results indicate that in the auxiliary discharge converters considered, a plasma potential drop  $V_P$  of the order of 0.2 to 0.3 V exists, at net emitter current densities of 5 to 10 A/cm<sup>2</sup>, with an emitter-collector spacing of 1 mm. The corresponding auxiliary discharge power expenditure for approximately optimum load current ( $I_L \simeq I_{L0} \simeq 1/2 I_L^{\max}$ , in our experiments) is of the order of 0.2 W/A of load current, with argon, for a favorable auxiliary emitter configuration. With xenon, this should become as low as 0.1 W/A, corresponding to an equivalent loss of output voltage of  $P_a/I_{L0} = 0.1$  V. Assuming that none of the ohmic electron heating power fed into the plasma by the resistive plasma potential drop  $V_P$  is recovered in the collector sheath (i. e., assuming  $I_L = I_{L0}$ ), the total power expended in plasma heating and ionization then is expressed by the sum of  $V_P$  and  $P_a/I_{L0}$ . The conclusion of our work so far is that this sum can be held to approximately 0.3 to 0.4 eV, for net emitter current densities of the order of 5 to 10 A/cm<sup>2</sup>, in the type of auxiliary discharge thermionic energy converter which we have investigated. This is an acceptable value and indicates the feasibility of this concept of thermionic energy conversion.

### Appendix

For the sake of completeness, the equations derived from the condition of conservation of electrons and applicable to the potential distribution of Fig. 3 are given below:

Equation (1) is replaced by

$$A_e J_{e\epsilon} \exp \left[ - \frac{e V_e}{k T_e} \right] = (A_e + A_c) \left( \frac{\epsilon n_{\epsilon} \bar{v}_{\epsilon}}{4} \right). \quad (1a)$$

Equation (2) is replaced by

$$I_L = \left( \frac{\epsilon n_{\epsilon} \bar{v}_{\epsilon}}{4} \right) A_c. \quad (2a)$$

Equations (3) to (6) remain unchanged; eq. (7) is replaced by eq. (2a), which may be rewritten

$$I_L = A_c J_{P\epsilon}. \quad (7a)$$

While the collector sheath potential does not appear explicitly in eq. (7a), it still is determined by eq. (7a) because  $J_{P\epsilon}$  is a function  $V_c$ .

### References

1. W. Bernstein, 21st Conf. on Physical Electronics, MIT, March 29, 1961
2. W. Bernstein and R. C. Knechtli, Proc. IRE 49, 1932 (December 1961).
3. Guthrie and Wakerling, Characteristics of Electrical Discharges in Magnetic Fields, McGraw-Hill, New York, 1949, Chap. II.
4. See Handbuch der Physik, Springer, New York, 1956, vol. 21, pp. 392-394.
5. L. Spitzer, Physics of Fully Ionized Gases, Interscience, New York, 1959, Chap. 5.
6. W. Bleakney, Phys. Rev. 36, 1303 (1930).
7. S. C. Brown, Basic Data of Plasma Physics, John Wiley and Sons, New York, 1959, pp. 102 and 111.
8. M. J. Druyvesteyn and F. M. Penning, Revs. Modern Phys. 12, 87 (1940).
9. D. Gabor, Nature 189, 868 (March 18, 1961); see Fig. 1.
10. M. Fox and R. C. Knechtli, Quarterly Status Report No. 1, Contract NAS 3-1909, p. 10, 1 September 1961 through 30 November 1961, Hughes Research Laboratories, Malibu, California.